arXiv:2002.07686v3 [cs.LG] 22 Oct 2020

Robust Quantization: One Model to Rule Them All

Moran Shkolnik [†°] **Brian Chmiel** [†°] **Ron Banner** [†]
Gil Shomron [°] **Yury Nahshan** [†] **Alex Bronstein** [°] **Uri Weiser** [°]

[†]Habana Labs – An Intel company, Caesarea, Israel,
[°]Department of Electrical Engineering - Technion, Haifa, Israel

{mshkolnik, bchmiel, rbanner, ynahshan}@habana.ai
gilsho@campus.technion.ac.il, bron@cs.technion.ac.il, uri.weiser@ee.technion.ac.il

Abstract

Neural network quantization methods often involve simulating the quantization process during training, making the trained model highly dependent on the target bit-width and precise way quantization is performed. Robust quantization offers an alternative approach with improved tolerance to different classes of data-types and quantization policies. It opens up new exciting applications where the quantization process is not static and can vary to meet different circumstances and implementations. To address this issue, we propose a method that provides intrinsic robustness to the model against a broad range of quantization processes. Our method is motivated by theoretical arguments and enables us to store a single generic model capable of operating at various bit-widths and quantization policies. We validate our method's effectiveness on different ImageNet models. A reference implementation accompanies the paper.

1 Introduction

Low-precision arithmetic is one of the key techniques for reducing deep neural networks computational costs and fitting larger networks into smaller devices. This technique reduces memory, bandwidth, power consumption and also allows us to perform more operations per second, which leads to accelerated training and inference.

Naively quantizing a floating point (FP32) model to 4 bits (INT4), or lower, usually incurs a significant accuracy degradation. Studies have tried to mitigate this by offering different quantization methods. These methods differ in whether they require training or not. Methods that require training (known as *quantization aware training* or QAT) simulate the quantization arithmetic on the fly [Esser et al., 2019, Zhang et al., 2018, Zhou et al., 2016], while methods that avoid training (known as *post-training quantization* or PTQ) quantize the model after the training while minimizing the quantization noise [Banner et al., 2019, Choukroun et al., 2019, Finkelstein et al., 2019, Zhao et al., 2019].

But these methods are not without disadvantages. Both create models sensitive to the precise way quantization is done (e.g., target bit-width). Krishnamoorthi [2018] has observed that in order to avoid accuracy degradation at inference time, it is essential to ensure that all quantization-related artifacts are faithfully modeled at training time. Our experiments in this paper further assess this observation. For example, when quantizing ResNet-18 [He et al., 2015] with DoReFa [Zhou et al., 2016] to 4 bits, an error of less than 2% in the quantizer step size results in an accuracy drop of 58%.

There are many compelling practical applications where quantization-robust models are essential. For example, we can consider the task of running a neural network on a mobile device with limited resources. In this case, we have a delicate trade-off between accuracy and current battery life, which can be controlled through quantization (lower bit-width => lower memory requirements => less

34th Conference on Neural Information Processing Systems (NeurIPS 2020), Vancouver, Canada.

energy). Depending on the battery and state of charge, a single model capable of operating at various quantization levels would be highly desirable. Unfortunately, current methods quantize the models to a single specific bit-width, experiencing dramatic degradations at all other operating points.

Recent estimates suggest that over 100 companies are now producing optimized inference chips [Reddi et al., 2019], each with its own rigid quantizer implementation. Different quantizer implementations can differ in many ways, including the rounding policy (e.g., round-to-nearest, stochastic rounding, etc), truncation policy, the quantization step size adjusted to accommodate the tensor range, etc. To allow rapid and easy deployment of DNNs on embedded low-precision accelerators, a single pre-trained generic model that can be deployed on a wide range of deep learning accelerators would be very appealing. Such a robust and generic model would allow DNN practitioners to provide a single off-the-shelf robust model suitable for every accelerator, regardless of the supported mix of data types, precise quantization process, and without the need to re-train the model on customer side.

In this paper, we suggest a generic method to produce robust quantization models. To that end, we introduce KURE — a KUrtosis REgularization term, which is added to the model loss function. By imposing specific kurtosis values, KURE is capable of manipulating the model tensor distributions to adopt superior quantization noise tolerance qualities. The resulting model shows strong robustness to variations in quantization parameters and, therefore, can be used in diverse settings and various operating modes (e.g., different bit-width).

This paper makes the following contributions: (i) we first prove that compared to the typical case of normally-distributed weights, uniformly distributed weight tensors have improved tolerance to quantization with a higher signal-to-noise ratio (SNR) and lower sensitivity to specific quantizer implementation; (ii) we introduce KURE — a method designed to uniformize the distribution of weights and improve their quantization robustness. We show that weight uniformization has no effect on convergence and does not hurt state-of-the-art accuracy before quantization is applied; (iii) We apply KURE to several ImageNet models and demonstrate that the generated models can be quantized robustly in both PTQ and QAT regimes.

2 Related work

Robust Quantization. Perhaps the work that is most related to ours is the one by Alizadeh et al. [2020]. In their work, they enhance the robustness of the network by penalizing the $L1-$norm of the gradients. Adding this type of penalty to the training objective requires computing gradients of the gradients, which requires running the backpropagation algorithm twice. On the other hand, our work promotes robustness by penalizing the fourth central moment (Kurtosis), which is differentiable and trainable through standard stochastic gradient methods. Therefore, our approach is more straightforward and introduces less overhead, while improving their reported results significantly (see Table 2 for comparison). Finally, our approach is more general. We demonstrate its robustness to a broader range of perturbations and conditions e.g., changes in quantization parameters as opposed to only changes to different bit-widths. In addition, our method applies to both post-training (PTQ) and quantization aware techniques (QAT) while [Alizadeh et al., 2020] focuses on PTQ.

Quantization methods. As a rule, these works can be classified into two types: post-training acceleration, and training acceleration. While post-training acceleration showed great successes in reducing the model weight's and activation to 8-bit, a more extreme compression usually involve with some accuracy degradation [Banner et al., 2019, Choukroun et al., 2019, Migacz, 2017, Gong et al., 2018, Zhao et al., 2019, Finkelstein et al., 2019, Lee et al., 2018, Nahshan et al., 2019]. Therefore, for 4-bit quantization researchers suggested fine-tuning the model by retraining the quantized model [Choi et al., 2018, Baskin et al., 2018, Esser et al., 2019, Zhang et al., 2018, Zhou et al., 2016, Yang et al., 2019, Gong et al., 2019, Elthakeb et al., 2019]. Both approaches suffer from one fundamental drawback - they are not robust to common variations in the quantization process or bit-widths other than the one they were trained for.

3 Model and problem formulation

Let $Q_\Delta(x)$ be a symmetric uniform M-bit quantizer with quantization step size Δ that maps a continuous value $x \in \mathbb{R}$ into a discrete representation

$$Q_\Delta(x) = \begin{cases} 2^{M-1}\Delta & x > 2^{M-1}\Delta \\ \Delta \cdot \left\lfloor \frac{x}{\Delta} \right\rceil & |x| \leq 2^{M-1}\Delta \\ -2^{M-1}\Delta & x < -2^{M-1}\Delta \,. \end{cases} \tag{1}$$

Given a random variable X taken from a distribution f and a quantizer $Q_\Delta(X)$, we consider the expected mean-squared-error (MSE) as a local distortion measure we would like to minimize, that is,

$$\text{MSE}(X, \Delta) = \mathbb{E}\left[(X - Q_\Delta(X))^2\right] . \tag{2}$$

Assuming an optimal quantization step $\tilde{\Delta}$ and optimal quantizer $Q_{\tilde{\Delta}}(X)$ for a given distribution X, we quantify the quantization sensitivity $\Gamma(X, \varepsilon)$ as the increase in $\text{MSE}(X, \Delta)$ following a small changes in the optimal quantization step size $\tilde{\Delta}(X)$. Specifically, for a given $\varepsilon > 0$ and a quantization step size Δ around $\tilde{\Delta}$ (i.e., $|\Delta - \tilde{\Delta}| = \varepsilon$) we measure the following difference:

$$\Gamma(X, \varepsilon) = \left| \text{MSE}(X, \Delta) - \text{MSE}(X, \tilde{\Delta}) \right| . \tag{3}$$

Lemma 1 *Assuming a second order Taylor approximation, the quantization sensitivity $\Gamma(X, \varepsilon)$ satisfies the following equation (the proof in Supplementary Material A.1.1):*

$$\Gamma(X, \varepsilon) = \left| \frac{\partial^2 \textit{MSE}(X, \Delta = \tilde{\Delta})}{\partial^2 \Delta} \cdot \frac{\varepsilon^2}{2} \right| . \tag{4}$$

We use Lemma 1 to compare the quantization sensitivity of the Normal distribution with and Uniform distribution.

3.1 Robustness to varying quantization step size

In this section, we consider different tensor distributions and their robustness to quantization. Specifically, we show that for a tensor X with a uniform distribution $Q(X)$ the variations in the region around $Q(X)$ are smaller compared with other typical distributions of weights.

Lemma 2 *Let X_U be a continuous random variable that is uniformly distributed in the interval $[-a, a]$. Assume that $Q_\Delta(X_U)$ is a uniform M-bit quantizer with a quantization step Δ. Then, the expected MSE is given as follows (the proof in Supplementary Material A.1.2):*

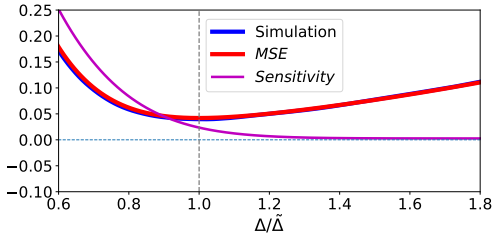
$$\textit{MSE}(X_U, \Delta) = \frac{(a - 2^{M-1}\Delta)^3}{3a} + \frac{2^M \cdot \Delta^3}{24a} . \tag{5}$$

In Fig. 1(b) we depict the MSE as a function of Δ value for 4-bit uniform quantization. We show a good agreement between Equation 5 and the synthetic simulations measuring the MSE.

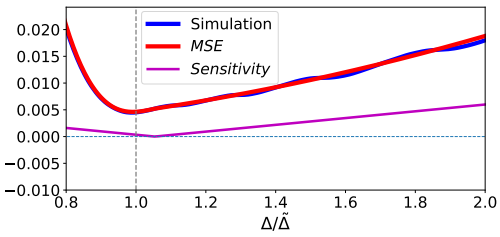
As defined in Eq. (3), we quantify the quantization sensitivity as the increase in MSE in the surrounding of the optimal quantization step $\tilde{\Delta}$. In Lemma 3 we will find $\tilde{\Delta}$ for a random variable that is uniformly distributed.

Lemma 3 *Let X_U be a continuous random variable that is uniformly distributed in the interval $[-a, a]$. Given an M-bit quantizer $Q_\Delta(X)$, the expected MSE is minimized by selecting the following quantization step size (the proof in Supplementary Material A.1.3):*

$$\tilde{\Delta} = \frac{2a}{2^M \pm 1} \approx \frac{2a}{2^M} . \tag{6}$$



(a) **Optimal quantization of normally distributed tensors.** The first order gradient zeroes at a region with a relatively high-intensity 2nd order gradient, i.e., a region with a high quantization sensitivity $\Gamma(X_N, \varepsilon)$. This sensitivity zeros only asymptotically when Δ (and MSE) tends to infinity. This means that optimal quantization is highly sensitive to changes in the quantization process.



(b) **Optimal quantization of uniformly distributed tensors.** First and second-order gradients zero at a similar point, indicating that the optimum $\tilde{\Delta}$ is attained at a region where quantization sensitivity $\Gamma(X_U, \varepsilon)$ tends to zero. This means that optimal quantization is tolerant and can bear changes in the quantization process without significantly increasing the MSE.

Figure 1: Quantization needs to be modeled to take into account uncertainty about the precise way it is being done. The best quantization that minimizes the MSE is also the most robust one with uniformly distributed tensors (b), but not with normally distributed tensors (a). **(i) Simulation:** 10,000 values are generated from a uniform/normal distribution and quantized using different quantization step sizes Δ. **(ii) MSE:** Analytical results, stated by Lemma 2 for the uniform case, and developed by [Banner et al., 2019] for the normal case - note these are in a good agreement with simulations. **(iii) Sensitivity:** second order derivative zeroes in the region with maximum robustness.

We can finally provide the main result of this paper, stating that the uniform distribution is more robust to modification in the quantization process compared with the typical distributions of weights and activations that tend to be normal.

Theorem 4 *Let X_U and X_N be continuous random variables with a uniform and normal distributions. Then, for any given $\varepsilon > 0$, the quantization sensitivity $\Gamma(X, \varepsilon)$ satisfies the following inequality:*

$$\Gamma(X_U, \varepsilon) < \Gamma(X_N, \varepsilon)\,, \tag{7}$$

*i.e., compared to the typical normal distribution, the uniform distribution is more robust to **changes** in the quantization step size Δ .*

Proof: In the following, we use Lemma 1 to calculate the quantization sensitivity of each distribution. We begin with the uniform case. We have presented in Lemma 2 the $\text{MSE}(X_U)$ as a function of Δ. Hence, since we have shown in Lemma 3 that optimal step size for X_U is $\tilde{\Delta} \approx \frac{a}{2^{M-1}}$ we get that

$$\Gamma(X_U, \varepsilon) = \left| \frac{\partial^2 \text{mse}(X_U, \Delta = \tilde{\Delta})}{\partial^2 \Delta} \cdot \frac{\varepsilon^2}{2} \right| = \frac{2^{2M-1}(a - 2^{M-1}\tilde{\Delta}) + 2^{M-2}\tilde{\Delta}}{a} \cdot \frac{\varepsilon^2}{2} = \frac{\varepsilon^2}{4}\,. \tag{8}$$

We now turn to find the sensitivity of the normal distribution $\Gamma(X_N, \varepsilon)$. According to [Banner et al., 2019], the expected MSE for the quantization of a Gaussian random variable $N(\mu = 0, \sigma)$ is as follows:

$$\text{MSE}(X_N, \Delta) \approx (\tau^2 + \sigma^2) \cdot \left[1 - \text{erf}\left(\frac{\tau}{\sqrt{2}\sigma}\right)\right] + \frac{\tau^2}{3 \cdot 2^{2M}} - \frac{\sqrt{2}\tau \cdot \sigma \cdot \text{e}^{-\frac{\tau^2}{2 \cdot \sigma^2}}}{\sqrt{\pi}}\,, \tag{9}$$

where $\tau = 2^{M-1}\Delta$.

To obtain the quantization sensitivity, we first calculate the second derivative:

$$\frac{\partial^2 \text{MSE}(X_N, \Delta = \tilde{\Delta})}{\partial^2 \Delta} = \frac{2}{3 \cdot 2^{2M}} - 2\,\text{erf}\left(\frac{2^{M-1}\tilde{\Delta}}{\sqrt{2}\sigma}\right) - 2\,. \tag{10}$$

We have three terms: the first is positive but not larger than $\frac{1}{6}$ (for the case of $M = 1$); the second is negative in the range $[-2, 0]$; and the third is the constant -2. The sum of the three terms falls in the

range $[-4, -\frac{11}{6}]$. Hence, the quantization sensitivity for normal distribution is at least

$$\Gamma(X_N, \varepsilon) = \left| \frac{\partial^2 \text{MSE}(X_N, \Delta = \tilde{\Delta})}{\partial^2 \Delta} \cdot \frac{\varepsilon^2}{2} \right| \geq \frac{11\varepsilon^2}{12} . \tag{11}$$

This clearly establishes the theorem since we have that $\Gamma(X_N, \varepsilon) > \Gamma(X_U, \varepsilon)$ ■

3.2 Robustness to varying bit-width sizes

Fig. 2 presents the minimum MSE distortions for different bit-width when normal and uniform distributions are optimally quantized. These optimal MSE values constitute the optimal solution of equations Eq. (5) and Eq. (9), respectively. Note that the optimal quantization of uniformly distributed tensors is superior in terms of MSE to normally distributed tensors at all bit-width representations.

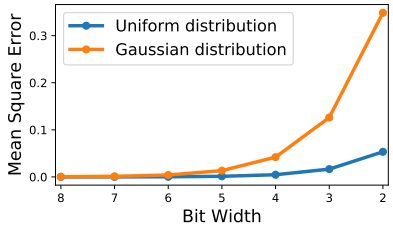


Figure 2: MSE as a function of bit-width for Uniform and Normal distributions. $\text{MSE}(X_U, \tilde{\Delta})$ is significantly smaller than $\text{MSE}(X_N, \tilde{\Delta})$.

3.3 When robustness and optimality meet

We have shown that for the uniform case optimal quantization step size is approximately $\tilde{\Delta} \approx \frac{2a}{2^M}$. The second order derivative is linear in Δ and zeroes at approximately the same location:

$$\Delta = \frac{2a}{2^M - \frac{1}{2^M}} \approx \frac{2a}{2^M} . \tag{12}$$

Therefore, for the uniform case, the optimal quantization step size in terms of $\text{MSE}(X, \tilde{\Delta})$ is generally the one that optimizes the sensitivity $\Gamma(X, \varepsilon)$, as illustrated by Fig. 1.

In this section, we proved that uniform distribution is more robust to quantization parameters than normal distribution. The robustness of the uniform distribution over Laplace distribution, for example, can be similarly justified. Next, we show how tensor distributions can be manipulated to form different distributions, and in particular to form the uniform distribution.

4 Kurtosis regularization (KURE)

DNN parameters usually follow Gaussian or Laplace distributions [Banner et al., 2019]. However, we would like to obtain the robust qualities that the uniform distribution introduces (Section 3). In this work, we use *kurtosis* — the fourth standardized moment — as a proxy to the probability distribution.

4.1 Kurtosis — The fourth standardized moment

The kurtosis of a random variable $\mathcal{X}$ is defined as follows:

$$\text{Kurt}\left[\mathcal{X}\right] = \mathbb{E}\left[\left(\frac{\mathcal{X} - \mu}{\sigma}\right)^4\right] , \tag{13}$$

where μ and σ are the mean and standard deviation of $\mathcal{X}$. The kurtosis provides a scale and shift-invariant measure that captures the shape of the probability distribution $\mathcal{X}$. If $\mathcal{X}$ is uniformly distributed, its kurtosis value will be 1.8, whereas if $\mathcal{X}$ is normally or Laplace distributed, its kurtosis values will be 3 and 6, respectively [DeCarlo, 1997]. We define "kurtosis target", $\mathcal{K}_T$, as the kurtosis value we want the tensor to adopt. In our case, the kurtosis target is 1.8 (uniform distribution).

4.2 Kurtosis loss

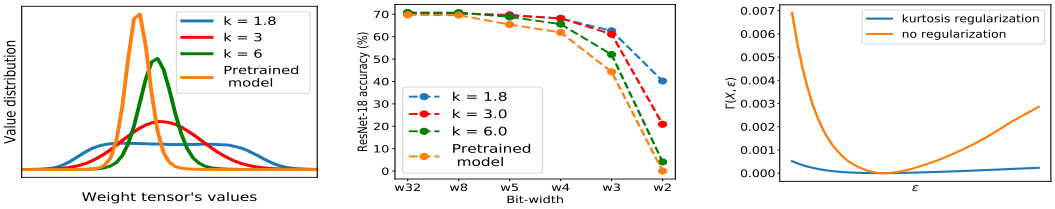
To control the model weights distributions, we introduce *kurtosis regularization* (KURE). KURE enables us to control the tensor distribution during training while maintaining the original model accuracy in full precision. KURE is applied to the model loss function, $\mathcal{L}$, as follows:

$$\mathcal{L} = \mathcal{L}_{\mathrm{p}} + \lambda \mathcal{L}_K \,, \tag{14}$$

$\mathcal{L}_p$ is the target loss function, $\mathcal{L}_K$ is the KURE term and λ is the KURE coefficient. $\mathcal{L}_K$ is defined as

$$\mathcal{L}_K = \frac{1}{L} \sum_{i=1}^{L} \left| \mathrm{Kurt}\left[\mathcal{W}_i\right] - \mathcal{K}_T \right|^2 \,, \tag{15}$$

where L is the number of layers and $\mathcal{K}_T$ is the target for kurtosis regularization.



(a) (b) (c)

Figure 3: (a) Weights distribution of one layer in ResNet-18 with different $\mathcal{K}_T$. (b) Accuracy of ResNet-18 with PTQ and different $\mathcal{K}_T$. (c) Weights sensitivity $\Gamma(X, \varepsilon)$ in one ResNet-18 layer as a function of change in the step size from the optimal quantization step size ($\varepsilon = |\Delta - \tilde{\Delta}|$).

We train ResNet-18 with different $\mathcal{K}_T$ values. We observe improved robustness for changes in quantization step size and bit-width when applying kurtosis regularization. As expected, optimal robustness is obtained with $\mathcal{K}_T = 1.8$. Fig. 3c demonstrates robustness for quantization step size. Fig. 3b demonstrates robustness for bit-width and also visualizes the effect of using different $\mathcal{K}_T$ values. The ability of KURE to control weights distribution is shown in Fig. 3a.

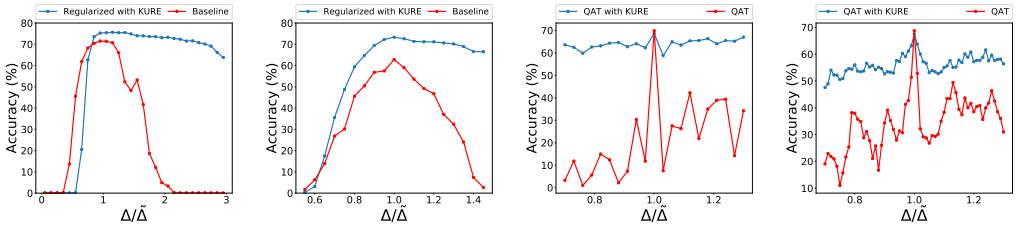
5 Experiments

In this section, we evaluate the robustness KURE provides to quantized models. We focus on robustness to bit-width changes and perturbations in quantization step size. For the former set of experiments, we also compare against the results recently reported by Alizadeh et al. [2020] and show significantly improved accuracy. All experiments are conducted using Distiller [Zmora et al., 2019], using ImageNet dataset [Deng et al., 2009] on CNN architectures for image classification (ResNet-18/50 [He et al., 2015] and MobileNet-V2 [Sandler et al., 2018]).

5.1 Robustness towards variations in quantization step size

Variations in quantization step size are common when running on different hardware platforms. For example, some accelerators require the quantization step size Δ to be a power of 2 to allow arithmetic shifts (e.g., multiplication or division is done with shift operations only). In such cases, a network trained to operate at a step size that is not a power of two, might result in accuracy degradation. Benoit et al. [2017] provides an additional use case scenario with a quantization scheme that uses only a predefined set of quantization step sizes for weights and activations.

We measure the robustness to this type of variation by modifying the optimized quantization step size. We consider two types of methods, namely, PTQ and QAT. Fig. 4a and Fig. 4b show the robustness of KURE in ResNet50 for PTQ based methods. We use the LAPQ method [Nahshan et al., 2019] to find the optimal step size. In Fig. 4c and Fig. 4d we show the robustness of KURE for QAT based method. Here, we train one model using the DoReFa method [Zhou et al., 2016] combined with KURE and compare its robustness against a model trained using DoReFa alone. Both models are trained to the same target bit-width (e.g., 4-bit weights and activations). Note that a slight change of 2% in the quantization step results in a dramatic drop in accuracy (from 68.3% to less than 10%). In contrast, when combined with KURE, accuracy degradation turns to be modest



(a) ResNet-50 with PTQ @ (W4,A8)

(b) ResNet-50 with PTQ @ (W3,A8)

(c) ResNet-18 with QAT @ (W4,A4)

(d) MobileNet-V2 with QAT @ (W4,A8)

Figure 4: The network has been optimized (either by using LAPQ method as our PTQ method or by training using DoReFa as our QAT method) for step size $\tilde{\Delta}$. Still, the quantizer uses a slightly different step size Δ. Small changes in optimal step size $\tilde{\Delta}$ of the weights tensors cause severe accuracy degradation in the quantized model. KURE significantly enhances the model robustness by promoting solutions that are more robust to uncertainties in the quantizer design. (a) and (b) show models quantized using PTQ method. (c) and (d) show models quantized with QAT method. @ (W,A) indicates the bit-width the model was quantized to.

5.2 Robustness towards variations in quantization bit-width

Here we test a different type of alteration. Now we focus on bit-width. We provide results related to QAT and PTQ as well as a comparison against [Alizadeh et al., 2020].

5.2.1 PTQ and QAT based methods

We begin with a PTQ based method (LAPQ - [Nahshan et al., 2019]) and test its performance when combined with KURE in Table 1. It is evident that applying KURE achieves better accuracy, especially in the lower bit-widths.

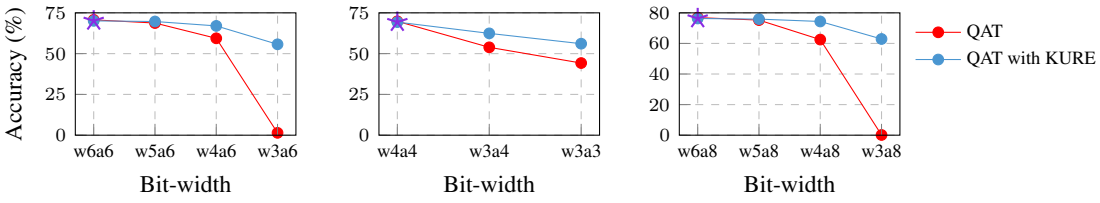
Table 1: KURE impact on model accuracy. (ResNet-18, ResNet-50 and MobileNet-V2 with ImageNet data-set)

			W/A configuration						
Model	Method	FP	4 / FP	3 / FP	2 / FP	6 / 6	5 / 5	4 / 4	3 / 3
ResNet-50	No regularization	76.1	71.8	62.9	10.3	74.8	72.9	70	38.4
	KURE regularization	76.3	**75.6**	**73.6**	**64.2**	**76.2**	**75.8**	**74.3**	**66.5**
ResNet-18	No regularization	69.7	62.6	52.4	0.5	68.6	65.4	59.8	44.3
	KURE regularization	70.3	**68.3**	**62.6**	**40.2**	**70**	**69.7**	**66.9**	**57.3**
MobileNet-V2	No regularization	71.8	60.4	31.8	–	69.7	64.6	48.1	3.7
	KURE regularization	71.3	**67.6**	**56.6**	–	**70**	**66.9**	**59**	**24.4**

Turning to QAT-based methods, Fig. 5 demonstrates the results with the LSQ quantization-aware method [Esser et al., 2019]. Additional results with different QAT methods can be found in the supplementary material.

5.2.2 A competitive comparison against [Alizadeh et al., 2020]

In Table 2 we compare our results to those reported by Alizadeh et al. [2020]. Our simulations indicate that KURE produces better accuracy results for all operating points (see Figure 2). It is worth mentioning that the method proposed by Alizadeh et al. [2020] is more compute-intensive than KURE since it requires second-order gradient computation (done through double-backpropagation), which has a significant computational overhead. For example, the authors mentioned in their work that their regularization increased time-per-epoch from 33:20 minutes to 4:45 hours for ResNet-18.



(a) ResNet-18 with QAT @ (W6,A6)

(b) ResNet-18 with QAT @ (W4,A4)

(c) ResNet-50 with QAT @ (W6,A8)

Figure 5: Bit-width robustness comparison of QAT model with and without KURE on different ImageNet architectures. We use LSQ method as our QAT method. The $\star$ is the original point to which the QAT model was trained. In (b) we change both activations and weights bit-width, while in (a) and (c) we change only the weights bit-width - which are more sensitive to quantization.

Table 2: Robustness comparison between KURE and [Alizadeh et al., 2020] for ResNet-18 on the ImageNet dataset.

		W/A configuration		
Method	FP32	8 / 8	6 / 6	4 / 4
L1 Regularization	70.07	69.92	66.39	0.22
L1 Regularization ($\lambda = 0.05$)	64.02	63.76	61.19	55.32
KURE (Ours)	**70.3**	**70.2**	**70**	**66.9**

6 Summary

Robust quantization aims at maintaining a good performance under a variety of quantization scenarios. We identified two important use cases for improving quantization robustness — robustness to quantization across different bit-widths and robustness across different quantization policies. We then show that uniformly distributed tensors are much less sensitive to variations compared to normally distributed tensors, which are the typical distributions of weights and activations. By adding KURE to the training phase, we change the distribution of the weights to be uniform-like, improving their robustness. We empirically confirmed the effectiveness of our method on various models, methods, and robust testing scenarios.

This work focuses on weights but can also be used for activations. KURE can be extended to other domains such as recommendation systems and NLP models. The concept of manipulating the model distributions with kurtosis regularization may also be used when the target distribution is known.

Broader Impact

Deep neural networks take up tremendous amounts of energy, leaving a large carbon footprint. Quantization can improve energy efficiency of neural networks on both commodity GPUs and specialized accelerators. Robust quantization takes another step and create one model that can be deployed across many different inference chips avoiding the need to re-train it before deployment (i.e., reducing CO2 emissions associated with re-training).

References

Milad Alizadeh, Arash Behboodi, Mart van Baalen, Christos Louizos, Tijmen Blankevoort, and Max Welling. Gradient $l1$ regularization for quantization robustness. *The International Conference on Learning Representations (ICLR)*, 2020.

Ron Banner, Yury Nahshan, Elad Hoffer, and Daniel Soudry. Post-training 4-bit quantization of convolution networks for rapid-deployment. *Conference on Neural Information Processing Systems (NeurIPS)*, 2019.

Chaim Baskin, Natan Liss, Yoav Chai, Evgenii Zheltonozhskii, Eli Schwartz, Raja Girayes, Avi Mendelson, and Alexander M Bronstein. Nice: Noise injection and clamping estimation for neural network quantization. *arXiv preprint arXiv:1810.00162*, 2018.

Jacob Benoit, Kligys Skirmantas, Chen Bo, Zhu Menglong, Tang Matthew, Howard Andrew, Adam Hartwig, and Kalenichenko Dmitry. Quantization and training of neural networks for efficient integer-arithmetic-only inference. *arXiv preprint arXiv:1712.05877*, 2017. URL `https://arxiv.org/abs/1712.05877`.

Jungwook Choi, Zhuo Wang, Swagath Venkataramani, Pierce I-Jen Chuang, Vijayalakshmi Srinivasan, and Kailash Gopalakrishnan. Pact: Parameterized clipping activation for quantized neural networks. *arXiv preprint arXiv:1805.06085*, 2018.

Yoni Choukroun, Eli Kravchik, and Pavel Kisilev. Low-bit quantization of neural networks for efficient inference. *arXiv preprint arXiv:1902.06822*, 2019.

Lawrence T. DeCarlo. "On the Meaning and Use of Kurtosis . *Psychological Methods, 2(3)*, page 292–307, 1997. URL `https://psycnet.apa.org/record/1998-04950-005`.

J. Deng, W. Dong, R. Socher, L.-J. Li, K. Li, and L. Fei-Fei. ImageNet: A Large-Scale Hierarchical Image Database. In *CVPR09*, 2009.

Ahmed T Elthakeb, Prannoy Pilligundla, and Hadi Esmaeilzadeh. SinReQ: Generalized sinusoidal regularization for automatic low-bitwidth deep quantized training. *arXiv preprint arXiv:1905.01416*, 2019.

Steven K. Esser, Jeffrey L. McKinstry, Deepika Bablani, Rathinakumar Appuswamy, and Dharmendra S. Modha. Learned step size quantization. *arXiv preprint arXiv:1902.08153*, 2019. URL `https://arxiv.org/abs/1902.08153`.

Alexander Finkelstein, Uri Almog, and Mark Grobman. Fighting quantization bias with bias. *arXiv preprint arXiv:1906.03193*, 2019.

Jiong Gong, Haihao Shen, Guoming Zhang, Xiaoli Liu, Shane Li, Ge Jin, Niharika Maheshwari, Evarist Fomenko, and Eden Segal. Highly efficient 8-bit low precision inference of convolutional neural networks with IntelCaffe. In *Proceedings of Reproducible Quality-Efficient Systems Tournament on Co-designing Pareto-efficient Deep Learning (ReQuEST)*, 2018.

Ruihao Gong, Xianglong Liu, Shenghu Jiang, Tianxiang Li, Peng Hu, Jiazhen Lin, Fengwei Yu, and Junjie Yan. Differentiable soft quantization: Bridging full-precision and low-bit neural networks. *arXiv preprint arXiv:1908.05033*, 2019. URL `http://arxiv.org/abs/1908.05033`.

Kaiming He, Xiangyu Zhang, Shaoqing Ren, and Jian Sun. Deep residual learning for image recognition, 2015.

Raghuraman Krishnamoorthi. Quantizing deep convolutional networks for efficient inference: A whitepaper, 2018.

Jun Haeng Lee, Sangwon Ha, Saerom Choi, Won-Jo Lee, and Seungwon Lee. Quantization for rapid deployment of deep neural networks. *arXiv preprint arXiv:1810.05488*, 2018. URL `http://arxiv.org/abs/1810.05488`.

Szymon Migacz. 8-bit inference with TensorRT. NVIDIA GPU Technology Conference, 2017.

Yury Nahshan, Brian Chmiel, Chaim Baskin, Evgenii Zheltonozhskii, Ron Banner, Alex M. Bronstein, and Avi Mendelson. Loss aware post-training quantization, 2019.

Vijay Janapa Reddi, Christine Cheng, David Kanter, Peter Mattson, Guenther Schmuelling, Carole-Jean Wu, Brian Anderson, Maximilien Breughe, Mark Charlebois, William Chou, Ramesh Chukka, Cody Coleman, Sam Davis, Pan Deng, Greg Diamos, Jared Duke, Dave Fick, J. Scott Gardner, Itay Hubara, Sachin Idgunji, Thomas B. Jablin, Jeff Jiao, Tom St. John, Pankaj Kanwar, David Lee, Jeffery Liao, Anton Lokhmotov, Francisco Massa, Peng Meng, Paulius Micikevicius, Colin Osborne, Gennady Pekhimenko, Arun Tejusve Raghunath Rajan, Dilip Sequeira, Ashish Sirasao, Fei Sun, Hanlin Tang, Michael Thomson, Frank Wei, Ephrem Wu, Lingjie Xu, Koichi Yamada, Bing Yu, George Yuan, Aaron Zhong, Peizhao Zhang, and Yuchen Zhou. Mlperf inference benchmark, 2019.

Mark Sandler, Andrew G. Howard, Menglong Zhu, Andrey Zhmoginov, and Liang-Chieh Chen. Inverted residuals and linear bottlenecks: Mobile networks for classification, detection and segmentation. *CoRR*, abs/1801.04381, 2018. URL http://arxiv.org/abs/1801.04381.

Jiwei Yang, Xu Shen, Jun Xing, Xinmei Tian, Houqiang Li, Bing Deng, Jianqiang Huang, and Xian-sheng Hua. Quantization networks. In *The IEEE Conference on Computer Vision and Pattern Recognition (CVPR)*, June 2019. URL http://openaccess.thecvf.com/content_CVPR_2019/html/Yang_Quantization_Networks_CVPR_2019_paper.html.

Dongqing Zhang, Jiaolong Yang, Dongqiangzi Ye, and Gang Hua. Lq-nets: Learned quantization for highly accurate and compact deep neural networks. In *The European Conference on Computer Vision (ECCV)*, September 2018. URL http://openaccess.thecvf.com/content_ECCV_2018/html/Dongqing_Zhang_Optimized_Quantization_for_ECCV_2018_paper.html.

Ritchie Zhao, Yuwei Hu, Jordan Dotzel, Christopher De Sa, and Zhiru Zhang. Improving neural network quantization using outlier channel splitting. *arXiv preprint arXiv:1901.09504*, 2019. URL https://arxiv.org/abs/1901.09504.

Shuchang Zhou, Zekun Ni, Xinyu Zhou, He Wen, Yuxin Wu, and Yuheng Zou. Dorefa-net: Training low bitwidth convolutional neural networks with low bitwidth gradients. *ArXiv*, abs/1606.06160, 2016.

Neta Zmora, Guy Jacob, Lev Zlotnik, Bar Elharar, and Gal Novik. Neural network distiller: A python package for dnn compression research. *arXiv preprint arXiv:1910.12232*, 2019. URL http://arxiv.org/abs/1910.12232.

A Supplementary Material

A.1 Proofs from section: Model and problem formulation

A.1.1

Lemma 1 *Assuming a second order Taylor approximation, the quantization sensitivity* $\Gamma(X,\epsilon)$ *satisfies the following equation:*

$$\Gamma(X,\epsilon) = \left| \frac{\partial^2 \mathit{MSE}(X, \Delta = \tilde{\Delta})}{\partial^2 \Delta} \cdot \frac{\epsilon^2}{2} \right| . \tag{A.1}$$

Proof: Let Δ' be a quantization step with similar size to $\tilde{\Delta}$ so that $|\Delta' - \tilde{\Delta}| = \epsilon$. Using a second order Taylor expansion, we approximate $\text{MSE}(X, \Delta')$ around $\tilde{\Delta}$ as follows:

$$\begin{aligned} \text{MSE}(X, \Delta') = \text{MSE}(X, \tilde{\Delta}) + \frac{\partial \text{MSE}(X, \Delta = \tilde{\Delta})}{\partial \Delta}(\Delta' - \tilde{\Delta}) \\ + \frac{1}{2} \cdot \frac{\partial^2 \text{MSE}(X, \Delta = \tilde{\Delta})}{\partial^2 \Delta}(\Delta' - \tilde{\Delta})^2 + O(\Delta' - \tilde{\Delta})^3 . \end{aligned} \tag{A.2}$$

Since $\tilde{\Delta}$ is the optimal quantization step for $\text{MSE}(X, \Delta)$, we have that $\frac{\partial \text{mse}(X, \Delta = \tilde{\Delta})}{\partial \Delta} = 0$. In addition, by ignoring order terms higher than two, we can re-write Equation (A.2) as follows:

$$\text{MSE}(X, \Delta') - \text{MSE}(X, \tilde{\Delta}) = \frac{1}{2} \cdot \frac{\partial^2 \text{MSE}(X, \Delta = \tilde{\Delta})}{\partial^2 \Delta}(\Delta' - \tilde{\Delta})^2 = \frac{\partial^2 \text{MSE}(X, \Delta = \tilde{\Delta})}{\partial^2 \Delta} \cdot \frac{\epsilon^2}{2} . \tag{A.3}$$

Equation (A.3) holds also with absolute values:

$$\Gamma(X,\epsilon) = \left| \text{MSE}(X, \Delta') - \text{MSE}(X, \tilde{\Delta}) \right| = \left| \frac{\partial^2 \text{MSE}(X, \Delta = \tilde{\Delta})}{\partial^2 \Delta} \cdot \frac{\epsilon^2}{2} \right| . \tag{A.4}$$

■

A.1.2

Lemma 2 *Let* X_U *be a continuous random variable that is uniformly distributed in the interval* $[-a, a]$*. Assume that* $Q_\Delta(X_U)$ *is a uniform* M*-bit quantizer with a quantization step* Δ*. Then, the expected MSE is given as follows:*

$$\mathit{MSE}(X_U, \Delta) = \frac{(a - 2^{M-1}\Delta)^3}{3a} + \frac{2^M \cdot \Delta^3}{24a} .$$

Proof: Given a finite quantization step size Δ and a finite range of quantization levels 2^M, the quanitzer truncates input values larger than $2^{M-1}\Delta$ and smaller than $-2^{M-1}\Delta$. Hence, denoting by τ this threshold (i.e., $\tau \triangleq 2^{M-1}\Delta$), the quantizer can be modeled as follows:

$$Q_\Delta(x) = \begin{cases} \tau & x > \tau \\ \Delta \cdot \left\lfloor \frac{x}{\Delta} \right\rceil & |x| \leq \tau \\ -\tau & x < -\tau . \end{cases} \tag{A.5}$$

Therefore, by the law of total expectation, we know that

$$\begin{aligned}
&\mathbb{E}\left[\left(x - Q_\Delta(x)\right)^2\right] = \\
&\mathbb{E}\left[\left(x-\tau\right)^2 \mid x > \tau\right] \cdot P\left[x > \tau\right] + \\
&\mathbb{E}\left[\left(x - \Delta \cdot \left\lfloor \tfrac{x}{\Delta} \right\rceil\right)^2 \mid |x| \leq \tau\right] \cdot P\left[|x| \leq \tau\right] + \\
&\mathbb{E}\left[\left(x+\tau\right)^2 \mid x < -\tau\right] \cdot P\left[x < -\tau\right] .
\end{aligned} \tag{A.6}$$

We now turn to evaluate the contribution of each term in Equation (A.6). We begin with the case of $x > \tau$, for which the probability density is uniform in the range $[\tau, a]$ and zero for $x > a$. Hence, the conditional expectation is given as follows:

$$\mathbb{E}\left[\left(x-\tau\right)^2 \mid x > \tau\right] = \int_\tau^a \frac{(x-\tau)^2}{a-\tau} \cdot dx = \frac{1}{3} \cdot (a-\tau)^2 . \tag{A.7}$$

In addition, since x is uniformly distributed in the range $[-a, a]$, a random sampling from the interval $[\tau, a]$ happens with a probability

$$P\left[x > \tau\right] = \frac{a-\tau}{2a} . \tag{A.8}$$

Therefore, the first term in Equation (A.6) is stated as follows:

$$\mathbb{E}\left[\left(x-\tau\right)^2 \mid x > \tau\right] \cdot P\left[x > \tau\right] = \frac{(a-\tau)^3}{6a} . \tag{A.9}$$

Since x is symmetrical around zero, the first and last terms in Equation (A.6) are equal and their sum can be evaluated by multiplying Equation (A.9) by two.

We are left with the middle part of Equation (A.6) that considers the case of $|x| < \tau$. Note that the qunatizer rounds input values to the nearest discrete value that is a multiple of the quantization step Δ. Hence, the quantization error, $e = x - \Delta \cdot \left\lfloor \frac{x}{\Delta} \right\rceil$, is uniformly distributed and bounded in the range $[-\frac{\Delta}{2}, \frac{\Delta}{2}]$. Hence, we get that

$$\mathbb{E}\left[\left(x - \Delta \cdot \left\lfloor \frac{x}{\Delta} \right\rceil\right)^2 \mid |x| \leq \tau\right] = \int_{-\frac{\Delta}{2}}^{\frac{\Delta}{2}} \frac{1}{\Delta} \cdot e^2 de = \frac{\Delta^2}{12} . \tag{A.10}$$

Finally, we are left to estimate $P\left[|x| \leq \tau\right]$, which is exactly the probability of sampling a uniform random variable from a range of 2τ out of a total range of $2a$:

$$P\left[|x| \leq \tau\right] = \frac{2\tau}{2a} = \frac{\tau}{a} . \tag{A.11}$$

By summing all terms of Equation (A.6) and substituting $\tau = 2^{M-1}\Delta$, we achieve the following expression for the expected MSE:

$$\mathbb{E}\left[\left(x - Q_\Delta(x)\right)^2\right] = \frac{(a-\tau)^3}{3a} + \frac{\tau}{a}\frac{\Delta^2}{12} = \frac{(a-2^{M-1}\Delta)^3}{3a} + \frac{2^M\Delta^3}{24a} . \tag{A.12}$$

■

A.1.3

Lemma 3 *Let X_U be a continuous random variable that is uniformly distributed in the interval $[-a, a]$. Given an M-bit quantizer $Q_\Delta(X)$, the expected MSE $\mathbb{E}\left[\left(X - Q_\Delta(X)\right)^2\right]$ is minimized by selecting the following quantization step size:*

$$\tilde{\Delta} = \frac{2a}{2^M \pm 1} \approx \frac{2a}{2^M} . \tag{A.13}$$

Proof: We calculate the roots of the first order derivative of Equation (A.12) with respect to Δ as follows:

$$\frac{\partial \text{MSE}(X_U, \Delta)}{\partial \Delta} = \frac{1}{a}\left(2^{M-3}\Delta^2 - 2^{M-1}\left(a - 2^{M-1}\Delta\right)^2\right) = 0\,. \tag{A.14}$$

Solving Equation (A.14) yields the following solution:

$$\tilde{\Delta} = \frac{2a}{2^M \pm 1} \approx \frac{2a}{2^M}\,. \tag{A.15}$$

■

A.2 Hyper parameters to reproduce the results in Section 5- Experiments

In the following section we describe the hyper parameters used in the experiments section. A fully reproducible code accompanies the paper.

A.2.1 Hyper parameters for Section 5.1- Robustness towards variations in quantization step size

In Table A.1 we describe the hyper-parameters used in Fig. 4a and Fig. 4b in section 5.1 in the paper. We apply KURE on a pre-trained model from torch-vision repository and fine-tune it with the following hyper-parameters. When training phase ends we quantize the model using PTQ (Post Training Quantization) quantization method. All the other hyper-parameters like momentum and w-decay stay the same as in the pre-trained model.

Table A.1: Hyper parameters for the experiments in section 5.1 - Robustness towards variations in quantization step size using PTQ methods

arch	kurtosis target ($\mathcal{K}_T$)	KURE coefficient (λ)	initial lr	lr schedule	batch size	epochs	fp32 accuracy
ResNet-50	1.8	1.0	1e-3	decays by a factor of 10 every 30 epochs	128	50	76.4

In Table A.2 we describe the hyper-parameters used in Fig. 4c and Fig. 4d in section 5.1 in the paper. We combine KURE with QAT method during the training phase with the following hyper-parameters.

Table A.2: Hyper parameters for experiments in section 5.1 - Robustness towards variations in quantization step size using QAT methods

arch	QAT method	quantization settings (W/A)	kurtosis target ($\mathcal{K}_T$)	KURE coefficient (λ)	initial lr	lr schedule	batch size	epochs	acc
ResNet-18	DoReFa	4 / 4	1.8	1.0	1e-4	decays by a factor of 10 every 30 epochs	256	80	68.3
MobileNet-V2	DoReFa	4 / 8	1.8	1.0	5e-5	lr decay rate of 0.98 per epoch	128	10	66.9

A.2.2 Hyper parameters for Section 5.2- Robustness towards variations in quantization bit-width

In Table A.3 we describe the hyper-parameters used in Table 1 in section 5.2.1 in the paper. We apply KURE on a pre-trained model from torch-vision repository and fine-tune it with the following hyper-parameters.

Table A.3: Hyper parameters for experiments in section 5.2 - Robustness towards variations in quantization bit-width using PTQ methods

architecture	kurtosis target ($\mathcal{K}_T$)	KURE coefficient (λ)	initial lr	lr schedule	batch size	epochs	fp32 accuracy
ResNet-18	1.8	1.0	0.001	decays by a factor of 10 every 30 epochs	256	83	70.3
ResNet-50					128	49	76.4
MobileNet-V2					256	83	71.3

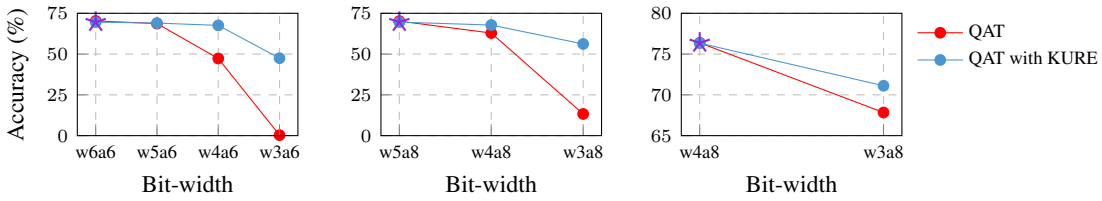
In Table A.4 we describe the hyper-parameters used in Fig. 5 in section 5.2.1 in the paper. We combine KURE with QAT method during the training phase with the following hyper-parameters.

Table A.4: Hyper parameters for experiments in section 5.2 - Robustness towards variations in quantization bit-width using QAT methods

arch	QAT method	quantization settings (W/A)	kurtosis target ($\mathcal{K}_T$)	KURE coefficient (λ)	initial lr	lr schedule	batch size	epochs	acc
ResNet-18	LSQ	6 / 6	1.8	1.0	1e-3	decays by a factor of 10 every 20 epochs	128	60	70.1
ResNet-18	LSQ	4 / 4					128	60	69.3
ResNet-50	LSQ	6 / 8					64	50	76.5

A.3 Robustness towards variations in quantization bit-width- additional results

In Fig. 5 in the paper we demonstrated robustness to variations in quantization bit-width of QAT models. we used LSQ method as our QAT model. In Fig. A.1 we demonstrate the improved robustness with different QAT methods (DoReFa and LSQ) and ImageNet models.



(a) ResNet-18 with DoReFa @ (W6,A6)

(b) ResNet-18 with DoReFa @ (W5,A8)

(c) ResNet-50 with LSQ @ (W4,A8)

Figure A.1: Bit-width robustness comparison of QAT model with and without KURE on different ImageNet architectures. The $\star$ is the original point to which the QAT model was trained.

A.4 Robustness towards variations in quantization step size- additional results

In section 5.1 in the paper, we explained the incentive to generate robust models for changes in the quantization step size. We mentioned that in many cases, accelerators support only a step size equal to a power of 2. In such cases, a model trained to operate at a step size different from a power of 2 value will suffer from a significant accuracy drop. Table A.5 shows the accuracy results when the quantization step size is equal to a power of 2 compared to the optimal step size ($\tilde{\Delta}$) , for ImageNet models trained with and without KURE.

A.5 Statistical significance of results on ResNet-18/ImageNet trained with DoReFa and KURE

Table A.5: KURE impact on model accuracy when rounding quantization step size to nearest power-of-2. (ResNet-18 and ResNet-50 with ImageNet data-set)

		W/A configuration			
		4 / FP		3 / FP	
Model	Method	$\Delta = \tilde{\Delta}$	$\Delta = 2^N$	$\Delta = \tilde{\Delta}$	$\Delta = 2^N$
ResNet-50	No regularization	71.8	63.6	62.9	53.2
	KURE regularization	**75.6**	**74.2**	**73.6**	**71.6**
ResNet-18	No regularization	62.6	61.4	52.4	37.5
	KURE regularization	**68.3**	**66.2**	**62.6**	**55.8**

Table A.6: Mean and standard deviation over multiple runs of ResNet-18 trained with DoReFa and KURE

architecture	QAT method	quantization settings (W/A)	Runs	Accuracy, % (mean $\pm$ std)
ResNet-18	DoReFa	4 / 4	3	(68.4 $\pm$ 0.09)

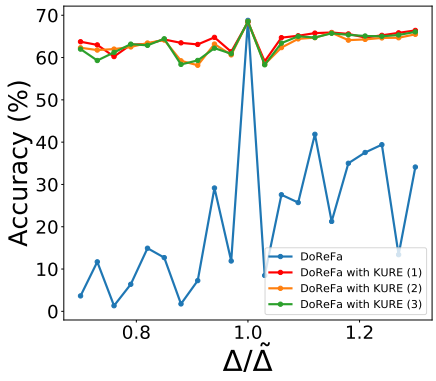


Figure A.2: The network has been trained for quantization step size $\tilde{\Delta}$. Still, the quantizer uses a slightly different step size Δ. Small changes in optimal step size $\tilde{\Delta}$ cause severe accuracy degradation in the quantized model. KURE significantly enhances the model robustness by promoting solutions that are more robust to uncertainties in the quantizer design (ResNet-18 on ImageNet).